TÜBİTAK

Turkish Journal of Physics

http://journals.tubitak.gov.tr/physics/

Research Article

Turk J Phys
(2015) 39: 1 – 15

doi:10.3906/fiz-1309-7

An approach to extract the parameters of solar cells from their illuminated $I-V$ curves using the Lambert W function

Ahmed A. EL TAYYAN*
Department of Physics, Al-Azhar University–Gaza, Gaza Strip, Palestine

Received: 27.09.2013 • **Accepted:** 02.06.2014 • **Published Online:** 23.02.2015 • **Printed:** 20.03.2015

Abstract: In this article an approach based on the Lambert W function is applied to analysis of various types solar cells and solar modules at a given insolation level and temperature; it can be used to extract accurate values of the parameters of a solar cell/module using experimental data or information available from the datasheet. These parameters are the photocurrent I_{ph}, the reverse saturation current I_o, the diode ideality factor a, the series resistance R_s, and the shunt resistance R_{sh}. The parameters I_o, a, R_s, and R_{sh} are calculated with the aid of 4 equations that can be solved simultaneously while increasing the value of I_{ph} in small increments. The calculated parameters are found to be in good agreement with those obtained in the literature. The experimental data of various solar cells/modules devices are obtained from the literature. Some of these devices are silicon solar cells and modules in addition to organic and DSSC solar cells. The mathematical $I-V$ characteristics and the mathematical $P-V$ characteristics are found to be in good agreement with the experimental data.

Key words: Solar cell, solar module, equivalent circuit, PV system modeling, Lambert W function

1. Introduction

Renewable energy generation systems, based on photovoltaic (PV) devices, present the most promising solutions for domestic power levels, to reduce CO_2 emissions and the energy consumption produced by gas and oil [1]. A PV system converts sunlight into electricity. The solar cell is the basic device of a PV system. Cells may be grouped to form modules or panels. Panels can be grouped to form large PV arrays. The cost and the performance of PV plants strongly depend on modules/arrays. However, the electrical parameters of the module/array, for example the short circuit current and the open circuit voltage, can be different than those provided by the manufacturer. Moreover, such parameters can change due to aging.

Solar cells' performance has been continuously improved through various intensive research efforts. Accurate knowledge of solar cells' parameters from experimental data is of vital importance in order to estimate their performance and to simulate, design, fabricate, and quality control the solar cells [2]. The electrical behavior of solar cells is usually described by the equivalent circuit of the single-diode model, the 2-diode model [3], or the 3-diode model [4,5]. Among these circuit models, the single-diode model (known also as the 5 parameters model) shown in Figure 1 has the simplest form. Although the single-diode model is simple, it can describe the electrical behavior of various solar cells well and satisfy most of their applications. Thus, the single-diode model has become the most widely used solar cell circuit model [6–23]. The relation between the

*Correspondence: ahmedtayyan@yahoo.com

current I and the voltage V in the single-diode model is given by

$$I = I_{ph} - I_0 \left\{ \exp\left[\frac{(V + IR_s)}{V_t a} \right] - 1 \right\} - \frac{V + IR_s}{R_{sh}}, \tag{1}$$

where I_{ph} and I_o are the photo-generated current and the dark saturation current of the PV system, respectively, $V_t = N_s kT/q$ is the thermal voltage of the PV system with N_s cells connected in series, R_s and R_{sh} are the cell series resistance and the cell shunt resistance, respectively, a is the diode quality factor, q is the electronic charge 1.6×10^{-19} C, k is the Boltzmann's constant $1.38 \times 10^{-23} J/K$, and T is the temperature in Kelvin.

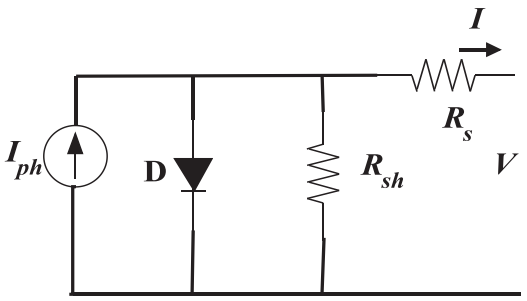

Figure 1. The single-diode model equivalent circuit of a PV device.

Many methods used to determine the unknown parameters I_{ph}, I_o, a, R_s, and R_{sh} have been the suggested by various authors [6–23]. Some authors use the measurements of illuminated $I-V$ characteristics at different illumination levels [6–8]. Others utilize dark and illuminated measurements [9–12]. However, the device parameters are widely influenced by the different illumination levels [13]. Therefore, it is crucially important to estimate all the parameters of a solar cell from a single $I-V$ curve (or some points on this curve) measured under constant illumination level. This is very important for the recently emerging organic solar cells, whose parameters are greatly influenced by different levels of illumination [14].

Ishibashi et al. have recently introduced a method to extract all the parameters of a solar cell under one constant illumination level [15]. However, this method relies on calculating the differential value dV/dI from the experimental data, which requires a very smooth $I-V$ curve. Thus, techniques to smooth the experimental data such as the polynomial approximation method are inevitable.

A widely used method to extract the solar cell parameters is the curve fitting approach [16–19]. The least squares approach, which is a common method used in curve fitting, extracts the parameters of a solar cell by minimizing the squared error between the calculated and the experimental data. However, the current in Eq. (1) constitutes an implicit function, i.e. it includes the dependent and independent variables (I, V) at the same time. This implicit nature of Eq. (1) increases the complexity and difficulty of the parameters' extraction.

An explicit analytic expression for I or V can be obtained with the help of the Lambert W function [20–25,27,28]. Jain et al. [20] have used the Lambert W function to study the properties of solar cells. However, their study is validated only on simulated $I-V$ characteristics instead of extracting the parameters from the experimental $I-V$ data. Later, Ortiz-Conde et al. [23] proposed a method to extract the solar cell parameters from the $I-V$ characteristics based on the Lambert W function. They first calculated the Co-content (CC) function from the exact explicit analytical expressions, and then extracted the device parameters by curve fitting [23]. However, the CC remains a function of I and V, and thus the fitting process is a bi-dimensional fitting

process. Another method to extract all the parameters of a solar cell from a single $I-V$ curve under constant illumination level using the Lambert W function has been suggested by Zhang et al. [24]. They have reduced the number of the parameters, so that the expression for I only depends on a, R_s, and R_{sh}. Then the analytic expression was directly used to fit the experimental data and extract the device parameters. Later Aazou and Assaid [25] determined the physical parameters of real photovoltaic solar cells without any approximation using MAPLE software [26]. Their work relied on the method proposed by Ortiz-Conde et al. [23]. Recently, a method to determine the values of R_s and R_{sh} at the maximum power point using a multivariable version of the Newton–Raphson technique has been proposed by Ghani and Duke [27]. In their work the equations that describe the behavior of the PV system are based on the Lambert W function. Later Ghani et al. [28] suggested a method to determine R_s, R_{sh} and a by modifying the method in Ghani and Duke [27].

In the present work, a new method to extract PV system parameters based on the Lambert W function and knowledge of the experimental data or the information available from the datasheet is described. It has been applied successfully to analysis of various types of solar cells and solar modules/arrays at a given insolation level and temperature.

2. Modeling of PV devices

The 5-parameter model Eq. (1) assumes that the dark current of a PV system can be described by a single exponential dependence modified by a diode quality factor a. The values of the 5 parameters in the equation must be determined in order to accurately reproduce the $I-V$ curve of a PV system. In principle, this requires 5 equations containing 5 unknowns that should be solved simultaneously to obtain the values of the parameters [29–31]. Eq. (1) is an implicit equation and cannot be solved analytically. However, an explicit form of current as a function of voltage, i.e. $I = f(V)$, can easily be obtained in terms of the Lambert W function using MAPLE software. This form is given by the following equation:

$$I = -\frac{V}{R_s} + \frac{aV_t}{R_s}\left(\begin{array}{l} -LambertW\left(\dfrac{R_s I_o R_{sh} \exp\left(\frac{R_{sh}\left(R_s I_{ph} + R_s I_o + V\right)}{aV_t\left(R_{sh}+R_s\right)} \right)}{aV_t\left(R_s+R_{sh}\right)} \right) \\ \\ + \frac{R_{sh}\left(R_s I_{ph} + R_s I_o + V\right)}{aV_t\left(R_{sh}+R_s\right)} \end{array} \right). \tag{2}$$

Another form $V = f(I)$ can easily be obtained in terms of the Lambert W function with the aid of MAPLE software. This form is given by the following equation:

$$V = -I\left(R_s + R_{sh}\right) + I_{ph}R_{sh} - aV_t LambertW\left(\frac{I_o R_{sh}}{aV_t} \exp\left(\frac{-R_{sh}\left(I - I_{ph} - I_o\right)}{aV_t} \right) \right) + I_o R_{sh}, \tag{3}$$

where $LambertW$ is the Lambert W function, which can be solved numerically. Eq. (2) has an analytical form and it is very convenient for use in computer programs to reproduce the $I-V$ curves of a solar cell when knowing all the parameters. However, this expression is still unsuitable for the purpose of extracting the device parameters [23]. When it is used in curve fitting to extract the device parameters, very large errors can be introduced. This is mainly caused by the very large difference between I_o and I_{ph} [24]. Although both I_o and I_{ph} are currents and have the same unit, the difference between their values is usually larger than 6 orders [24].

At short circuit condition, i.e. at $I = I_{sc}$, we have $V = 0$; thus Eq. (2) becomes

$$I_{sc} = \frac{aV_t}{R_s}\left(-LambertW\left(\frac{R_s I_o R_{sh}}{aV_t\left(R_{sh}+R_s\right)} \exp\left(\frac{R_{sh}\left(R_s I_{ph} + R_s I_o\right)}{aV_t\left(R_{sh}+R_s\right)} \right) \right) \right) + \frac{R_{sh}\left(I_{ph}+I_o\right)}{R_{sh}+R_s}. \tag{4}$$

At open circuit condition $V = V_{oc}$ we have $I = 0$; thus Eq. (3) becomes

$$V_{oc} = R_{sh}\left(I_{ph} + I_o\right) - aV_t LambertW\left(\frac{I_o R_{sh}}{aV_t}\exp\left(\frac{R_{sh}\left(I_{ph} + I_o\right)}{aV_t}\right)\right). \tag{5}$$

At the maximum power point $V = V_{mp}$, $I = I_{mp}$ Eq. (2) has the following form:

$$I_{mp} = \frac{1}{R_s}\left(\begin{array}{l} -V_{mp} + \left(-aV_t LambertW\left(\frac{I_o R_{sh} R_s}{aV_t(R_{sh}+R_s)}\exp\left(\frac{R_{sh}(R_s I_{ph}+R_s I_o+V_{mp})}{aV_t(R_{sh}+R_s)}\right)\right)\right) \\ +\frac{R_{sh}(R_s I_{ph}+R_s I_o+V_{mp})}{R_{sh}+R_s} \end{array}\right) \tag{6}$$

Multiplying both sides of Eq. (2) by V, the power $P(V)$ is obtained as

$$P(V) = \frac{V}{R_s}\left(-V - aV_t\left(\begin{array}{l} LambertW\left(\frac{I_o R_{sh} R_s}{aV_t(R_{sh}+R_s)}\exp\left(\frac{R_{sh}(R_s I_{ph}+R_s I_o+V)}{aV_t(R_{sh}+R_s)}\right)\right) \\ -\frac{R_{sh}(R_s I_{ph}+R_s I_o+V)}{aV_t(R_{sh}+R_s)} \end{array}\right)\right). \tag{7}$$

An additional equation can be derived from Eq. (7) using the fact that on the $P-V$ characteristics of a PV system at the maximum power point the derivative of power with respect to voltage is zero. Thus, by differentiating Eq. (7) with respect to V and evaluating $dP(V)/dV = 0$ at the maximum power point $(V = V_{mp},\ I = I_{mp})$ one gets Eq. (8):

$$\left(\frac{dP(V)}{dV}\right)_{V_{mp}} = 0. \tag{8}$$

Similarly, one can obtain the power P as a function of I as

$$P\left(I\right) = I\left(-R_s I - IR_{sh} + I_{ph}R_{sh} - aV_t LambertW\left(\frac{I_o R_{sh}}{aV_t} exp\left(\frac{-R_{sh}\left(I - I_{ph} - I_o\right)}{aV_t}\right)\right) + I_o R_{sh}\right). \tag{9}$$

A new additional equation can be obtained using the fact that on the $P-I$ characteristics of a PV system at the maximum power point the derivative of power with respect to current is zero. Thus, by differentiating Eq. (9) with respect to I and evaluating $dP(I)/dI = 0$ at the maximum power point $(V = V_{mp},\ I = I_{mp})$ one gets Eq. (10):

$$\left(\frac{dP(I)}{dI}\right)_{I_{mp}} = 0. \tag{10}$$

The final expressions of Eq. (8) and Eq. (10) are omitted due to lack of space. In principle, solving Eqs. (4), (5), (6), (8), and (10) simultaneously will give the values of the 5 unknown parameters. However, this approach is still unsuitable for the purpose of extracting the device parameters. This is mainly caused by the very large value difference between I_o and I_{ph}. Recalling that I_{ph} is slightly larger than I_{sc}, one can try solving simultaneously any subset of 4 equations from a set of 5 equations (Eqs. (4), (5), (6), (8), and (10)) to obtain values of I_o, a, R_s, and R_{sh} while increasing the value of I_{ph} in small steps starting from the I_{sc} value. This can be achieved easily by a simple *do loop*. MAPLE's *fsolve* command, which is a powerful tool to numerically compute a system of simultaneous equations, is used to find the unknown parameters. The algorithm of the method proposed to determine the values of I_{ph}, $I_{o,}a$, R_s, and R_{sh} is summarized by Figure 2. More details on the current approach to calculate the parameters will be presented in the next section when discussing the Si (RTC France) silicon solar cell.

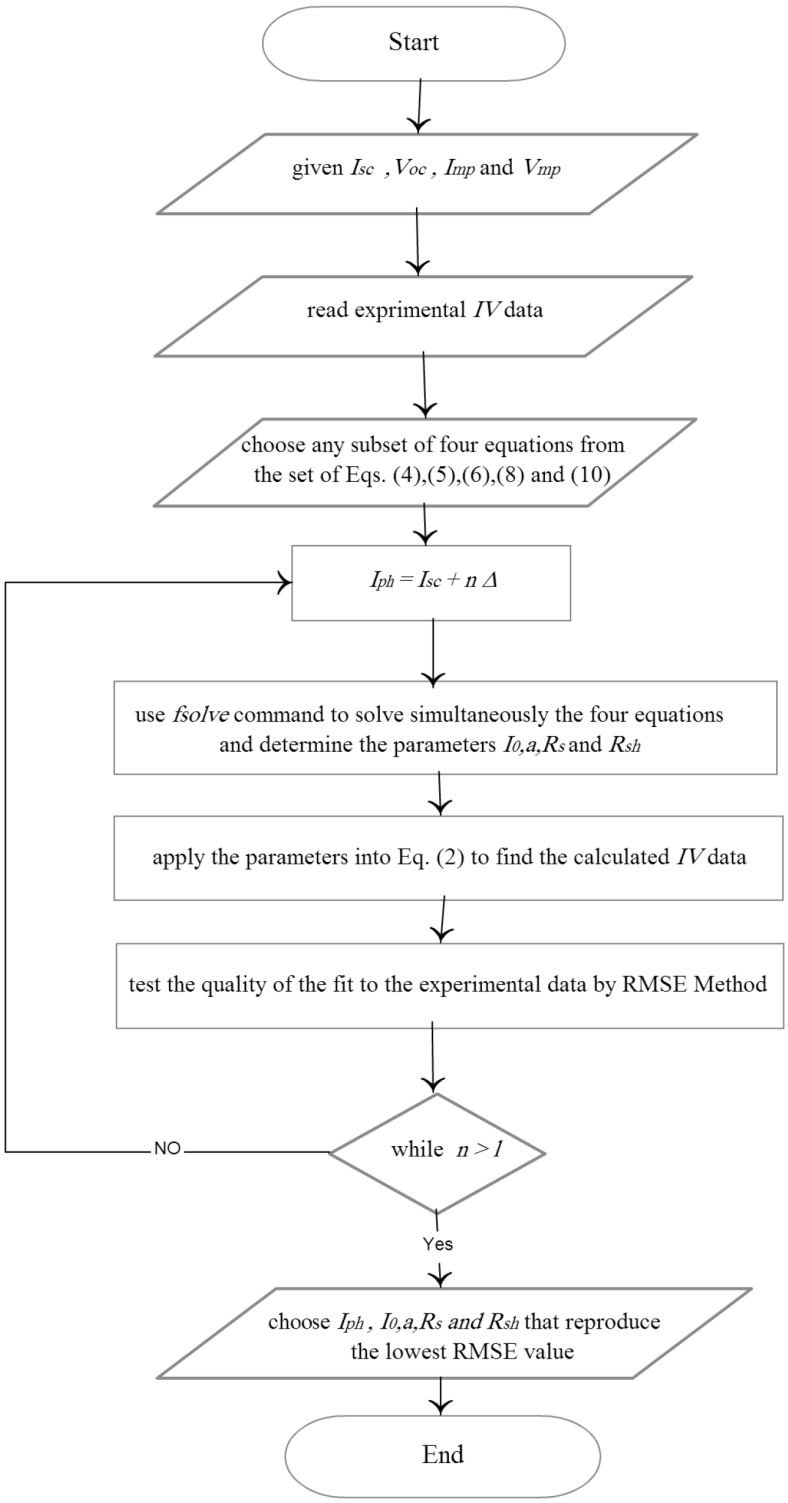

Figure 2. An algorithm of the proposed method to determine the values of I_{ph}, I_o, a, R_s, and R_{sh}.

3. Results and discussion

From the modeling section, it can be seen that the proposed method relies on values of I_{sc}, V_{oc}, I_{mp}, and V_{mp} being known. Normally, the values of I_{sc}, V_{oc}, I_{mp}, and V_{mp} can be obtained directly from the manufacturer's data sheet or from the experimental data [15]. However, sometimes the $I-V$ characteristics are only measured in the "active" quadrant of the solar cell without even measuring I_{sc}, V_{oc}, I_{mp}, and V_{mp} directly, or sometimes the density of the points is not sufficient to unambiguously determine their values. Under such condition, I_{sc}, V_{oc}, I_{mp}, and V_{mp} can be obtained by interpolation method or derived from the approximate $I-V$ polynomial expression [15]. Thus, I_{sc}, V_{oc}, I_{mp}, and V_{mp} can be determined to a high degree of accuracy for most cases and then the proposed method can be used. In this work, values of I_{sc}, V_{oc}, I_{mp}, and V_{mp} corresponding to various PV systems were obtained from the literature (see Table 1). On the other hand, the experimental $I-V$ data were deduced from the published literature using imageDIG digitizing software except for the $I-V$ data of MSX60 module, which is available online [32].

Table 1. Values of I_{sc}, V_{oc}, I_{mp}, and V_{mp} corresponding to solar cells and modules used in this work.

PV system	I_{sc} A	V_{oc} V	I_{mp} A	V_{mp} V	N_s	T°C
RTC Si solar cell [a]	0.760	0.5728	0.69119	0.45	1	33
Si Photowatt PWP201 module [a]	1.03	16.778	0.89789	12.6	36	45
MSX60 module [b]	3.81	21.1	3.50	17.14	36	25
KC200GT module [c]	8.21	32.9	7.61	26.3	54	25
Organic solar cell [d]	0.0046	1.2	0.00336	0.8	1	20
DSSC solar cell [e]	0.0021	0.7	0.00169	0.51	1	20

[a] See Ref. 16, [b] See Ref. 28, [c] See Ref. 34, [d] See Ref. 15, [e] See Ref. 19.

The single-diode model in Eq. (1) can describe not only the $I-V$ characteristics of standalone solar cells but also the electrical properties of multijunction solar cells, modules, and arrays where the cells are connected in series and/or parallel. Various types of solar cells have different properties. To test the validity of the proposed method, it will be applied to extract the parameters from the experimental data of various solar cells and modules. These devices include a silicon solar cell, silicon solar modules, an organic solar cell, and a dye sensitized solar cell (DSSC).

3.1. Application to a silicon solar cell

The proposed method is applied first to extract the parameters values of a 57-mm-diameter commercial Si (RTC France) silicon solar cell at 33 °C [16]. The parameters extracted by the current method are summarized and compared with published values in Table 2. Figure 3a illustrates a comparison between the corresponding $I-V$ curve reconstructed using the extracted parameters and the experimental data related to the same device. It is clear that the theoretical curve (solid line) is in very good agreement with the experimental data (points).

The mathematical and experimental variations of power with voltage for the Si (RTC France) silicon solar cell at 33 °C are illustrated in Figure 3b. The absolute errors between the calculated and the experimental current and power as a function of voltage are shown in Figure 3c. It can be seen that the absolute errors of the current and the power turn out to be insignificant but they tend to increase near the open circuit voltage.

Table 2. Extracted parameters by the current method and the previous work of various solar cells and solar modules.

Cell or module/array	I_{ph} (A)	I_o (μA)	$R_s(\Omega)$	R_{sh} (kΩ)	a
Si (RTC France)					
Previous work [a]	0.7608	0.3223	0.0364	0.0538	1.484
Previous work [b]	0.7609	0.4039	0.0364	0.0495	1.504
Previous work [c]	0.77	0.2	1.037	0.032	1.4
Previous work [d]	0.7611	0.2422	0.0373	0.042	1.4561
This work	0.7605	0.209	0.0403	0.0613	1.4391
Si Potowatt PWP201					
Previous work [a]	1.0318	3.2876	1.2057	0.549	1.346
Previous work [b]	1.0359	6.77	1.146	0.2	1.426
Previous work [c]	1	2.3	1.3	0.83	1.306
Previous work [d]	1.0332	1.597	1.313	0.6023	1.274
This work	1.033	4.1883	1.2263	0.4219	1.3742
MSX60 solar module					
Previous work[e]	3.812	0.1866	0.178	0.358569	1.358
This work	3.813	0.0645	0.2165	0.274937	1.277
KC200GT solar module					
Previous work[e]	8.215	0.04812	0.247	0.41489	1.235
Previous work[f]	8.21	0.09825	0.221	0.415405	1.3
This work	8.214	0.69127	0.239	0.490218	1.277
Organic solar cell					
Previous work[c]	0.0047	0.92	48	1.4	5.8
This work	0.0048	0.323	46.38	1.0741	5.0877
DSSC solar cell					
Previous work[g]	—	0.035	43.8	3.736	2.5
Previous work [c]	0.0021	0.023	42	3.2	2.5
Previous work[d]	0.002085	0.015143	44.7	3.285	2.3865
This work	0.00212	0.078626	25.729	2.714	2.7525

[a] See Ref. 16, [b] See Ref. 17, [c] See Ref. 15, [d] See Ref. 24, [e] See Ref. 31, [f] See Ref. 33, [g] See Ref. 19.

As mentioned before, the MAPLE *fsolve* command was used to solve simultaneously any subset of 4 equations from the set of 5 equations (Eqs. (4), (5), (6), (8), and (10)). A simple *do loop* can be used to search for solutions of I_o, a, R_s, and R_{sh} by varying the value of I_{ph} in steps according to the following formula:

$$I_{ph} = I_{sc} + n \cdot \Delta, \tag{11}$$

where n = 0,1,2,3,. . . . . ,l. Here, Δ is a small increment of current, and l is the number of iterations performed by the *do loop*.

For the (RTC France) solar cell, $I_{sc} = 0.760$ A, one started looking for simultaneous solutions by assigning $l = 18$ and $\Delta = 0.0001$ A. Solutions were started to be found at $n = 2$ and ended at $n = 16$. Figure 4 illustrates the variations of I_o, a, R_s, and R_{sh} with respect to the incremental increase in I_{ph}. In order to choose the most accurate values of the parameters I_{ph}, I_o, a, R_s, and R_{sh}, we apply them to Eq. (2) and then test the quality of the fit to the experimental data by performing statistical analysis. In this work, one of the fundamental measures of accuracy, the root mean squared error (RMSE), is used. The RMSE is given by

$$RMSE = \sqrt{\frac{\sum_1^m \left(I_{model} - I_{exp}\right)^2}{m}}, \tag{12}$$

where I_{model} and I_{exp} are the calculated and the measured currents for each value of voltage, respectively, and m is the number of data points. The most accurate set of the parameters I_{ph}, I_o, a, R_s, and R_{sh} is the set that can reproduce the $I-V$ characteristics when applied to Eq. (2) with the lowest RMSE value. The current method reveals that the most accurate I_{ph}, I_o, a, R_s, and R_{sh} values for the RTC solar cell are those listed in Table 2. The calculated values of the parameters I_{ph}, I_o, a, R_s, and R_{sh} are very close to those published in the literature except for R_s in Ishibashi et al. [15], which is larger than the value determined by this method or reported by others (see Table 2). The absolute errors of the calculated I_o, a, R_s, and R_{sh} with increasing I_{ph} are depicted in Figure 5.

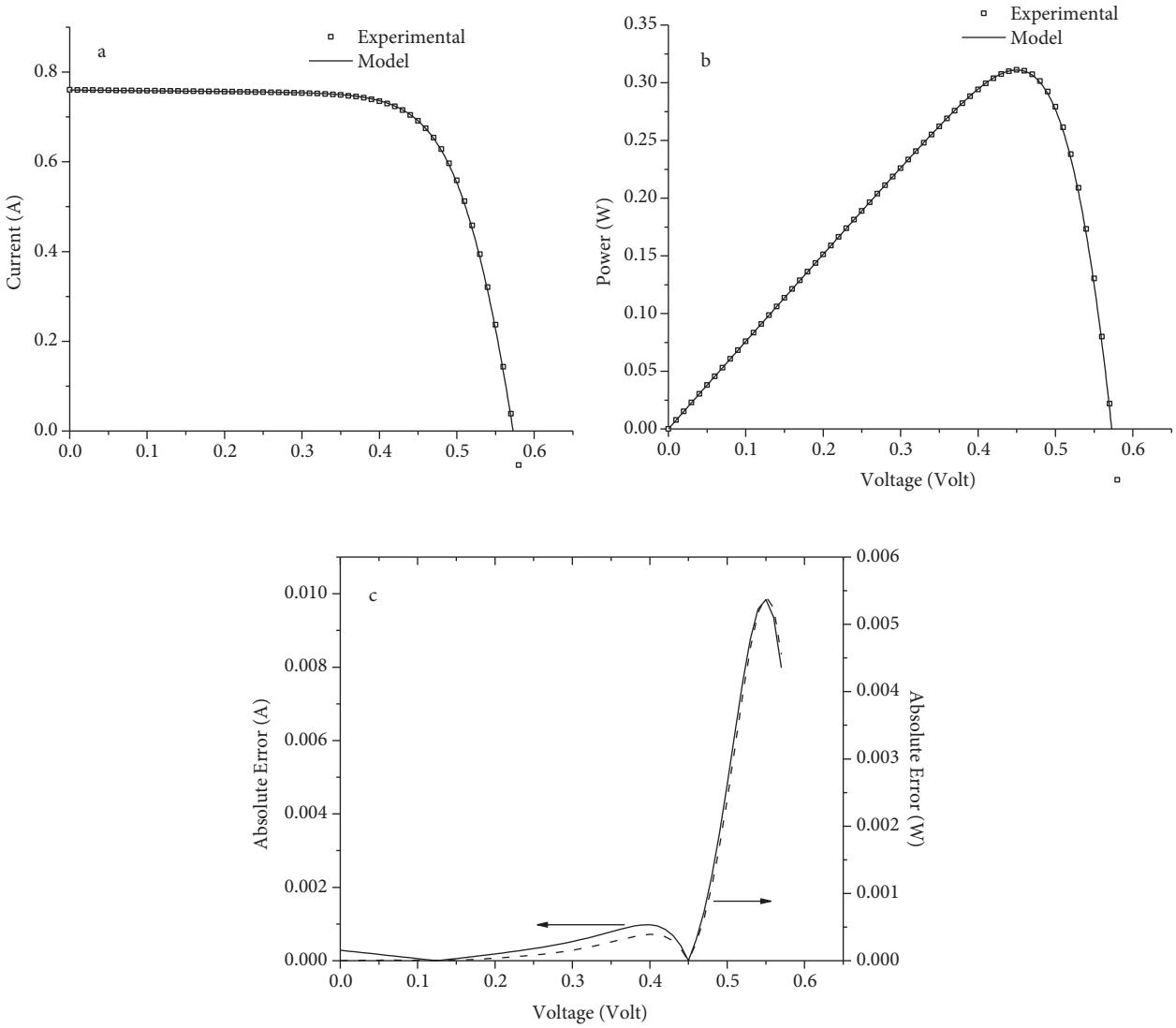

Figure 3. Si (RTC France) solar cell at 33 °C, 1000 W/m^2. (a) $I-V$ characteristics. (b) $P-V$ characteristics. (c) The variations of absolute errors of current and power with respect to voltage. In (a) and (b) points are experimental data, line is calculated data.

In the above, the sensitivity and the robustness of the proposed method have been discussed. In the following, we will not discuss them again but just apply them to various solar cells and modules.

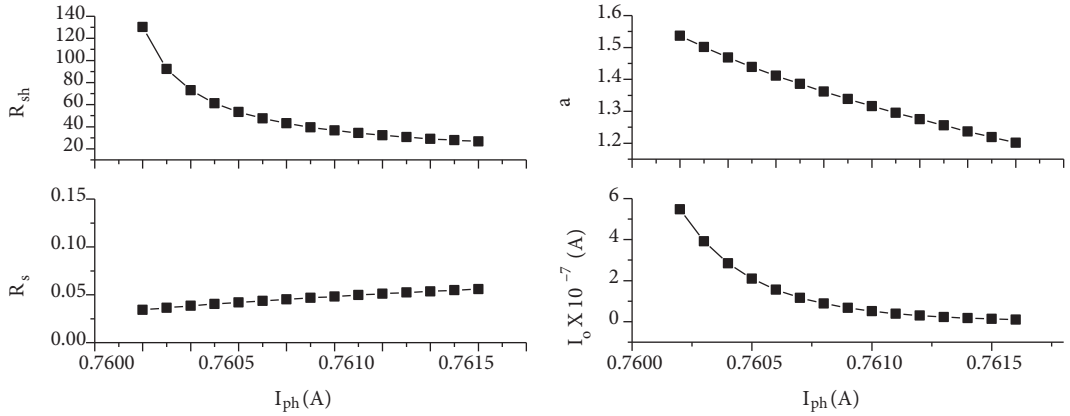

Figure 4. Variations of I_o, a, R_s,and R_{sh} with respect to incremental increase in I_{ph}.

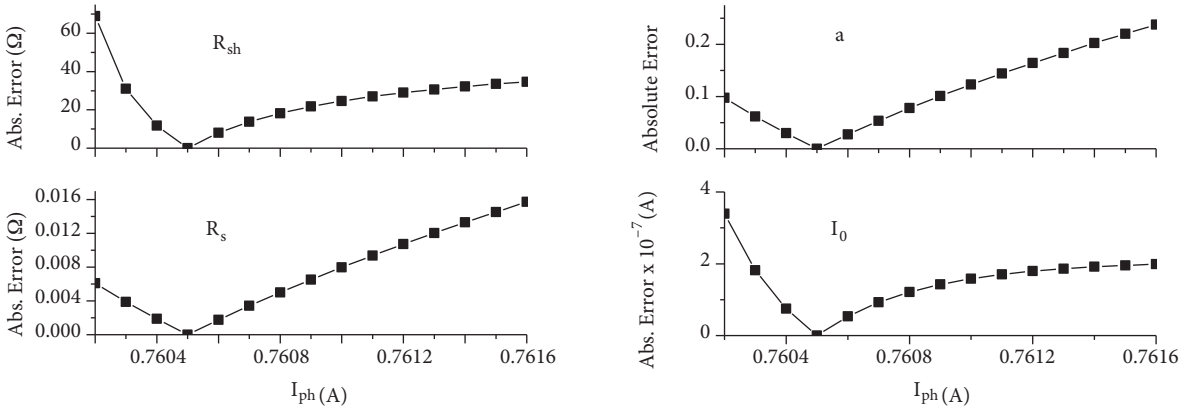

Figure 5. The absolute errors of I_o, a, R_s, and R_{sh} with incremental increase in I_{ph}.

3.2. Applications to silicon solar modules

3.2.1. Photowatt-PWP 201 module

The parameters of a silicon solar module (Photowatt-PWP 201) in which 36 polycrystalline silicon cells are connected in series are also investigated by the proposed method and the results are shown in Table 2. The measured $I-V$ data of the Photowatt-PWP 201 solar module are taken from Easwarakhanthan et al. [16]. Figure 6a illustrates the experimental data of the solar module (points) and the calculated $I-V$ curves using the parameters extracted in this work (solid line). One previous work [15] gave a low value of I_{ph} and thus a low value of I_{sc} (see Tables 1 and 2). This may be attributed to using only a small part of the experimental data far from the short circuit point, and thus some information from the experimental data is lost. Another previous study [17] gave a smaller value of R_{sh} and a larger value of a (see Table 2). This will cause a deviation between the calculated and the experimental curves.

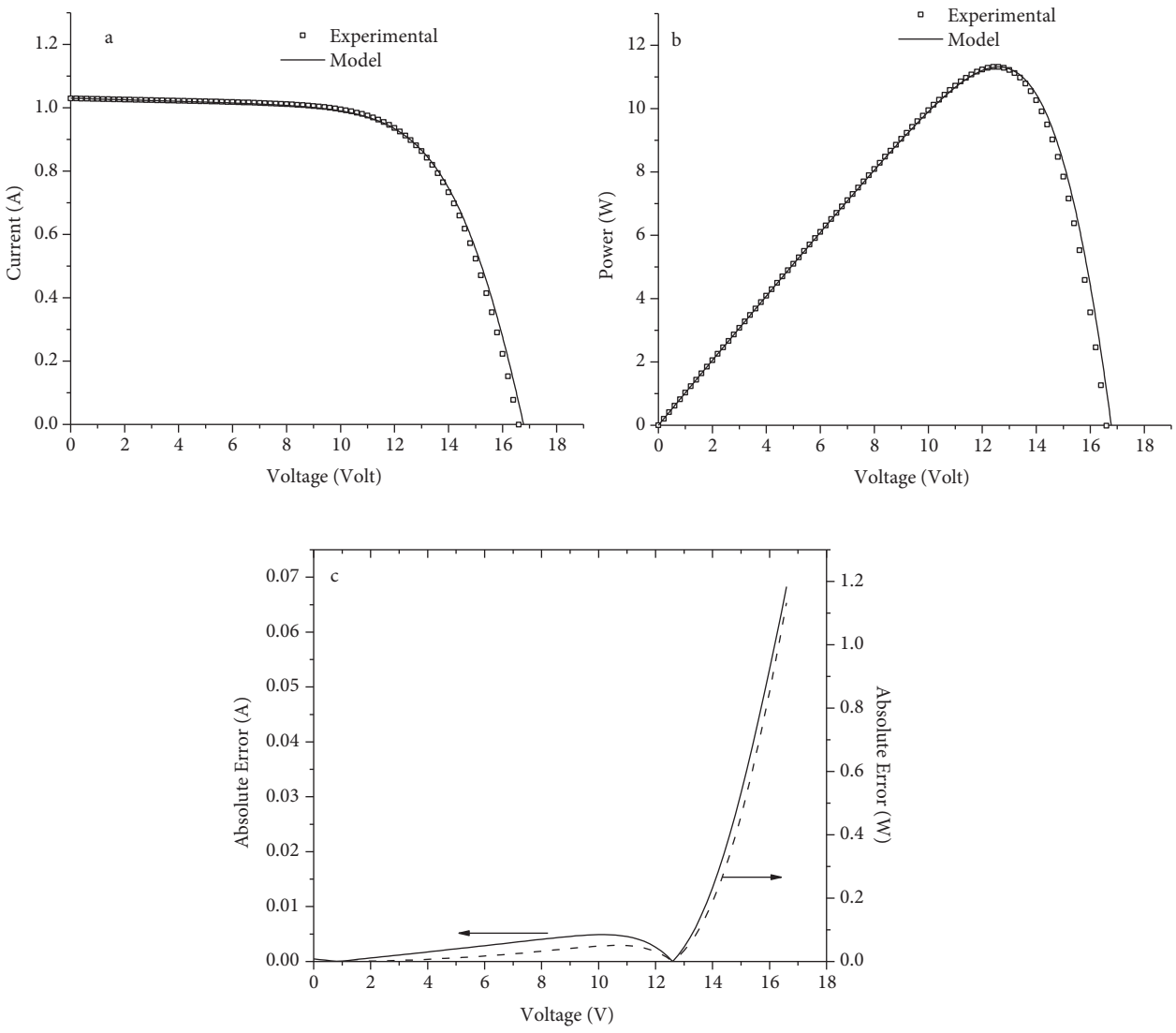

Figure 6. Photowatt-PWP 201 Si module at 45 °C, 1000 W/m^2. (a) Current–voltage curves. (b) Power–voltage curves. (c) Absolute errors of current and power variations with respect to voltage. In (a) and (b) points are experimental data, line is calculated data.

The $P-V$ characteristics and the variations of absolute errors of current and power with respect to voltage are shown in Figures 6b and 6c, respectively.

3.2.2. MSX60 module

Due to its wide use in traditional photovoltaic applications, the Solarex MSX60 PV module was chosen for modeling by the proposed method. The MSX60 module provides 60 W of nominal maximum power, and has 36 series of connected polycrystalline silicon cells. The key specifications I_{sc}, V_{oc}, I_{mp}, and V_{mp} are listed in Table 1.

The current method is implemented to the PV module and the values of the parameters I_{ph}, I_o, a, R_s, and R_{sh} are listed in Table 2. The experimental data points shown in Figure 7a are taken directly from the manufacturer's published curves [32]. The model curve matches the experimental data well. Figure 7b shows

the power–voltage curve. Again the discrete experimental data points show good correspondence to the model. Figure 7c also shows the absolute errors of current and power with respect to voltage.

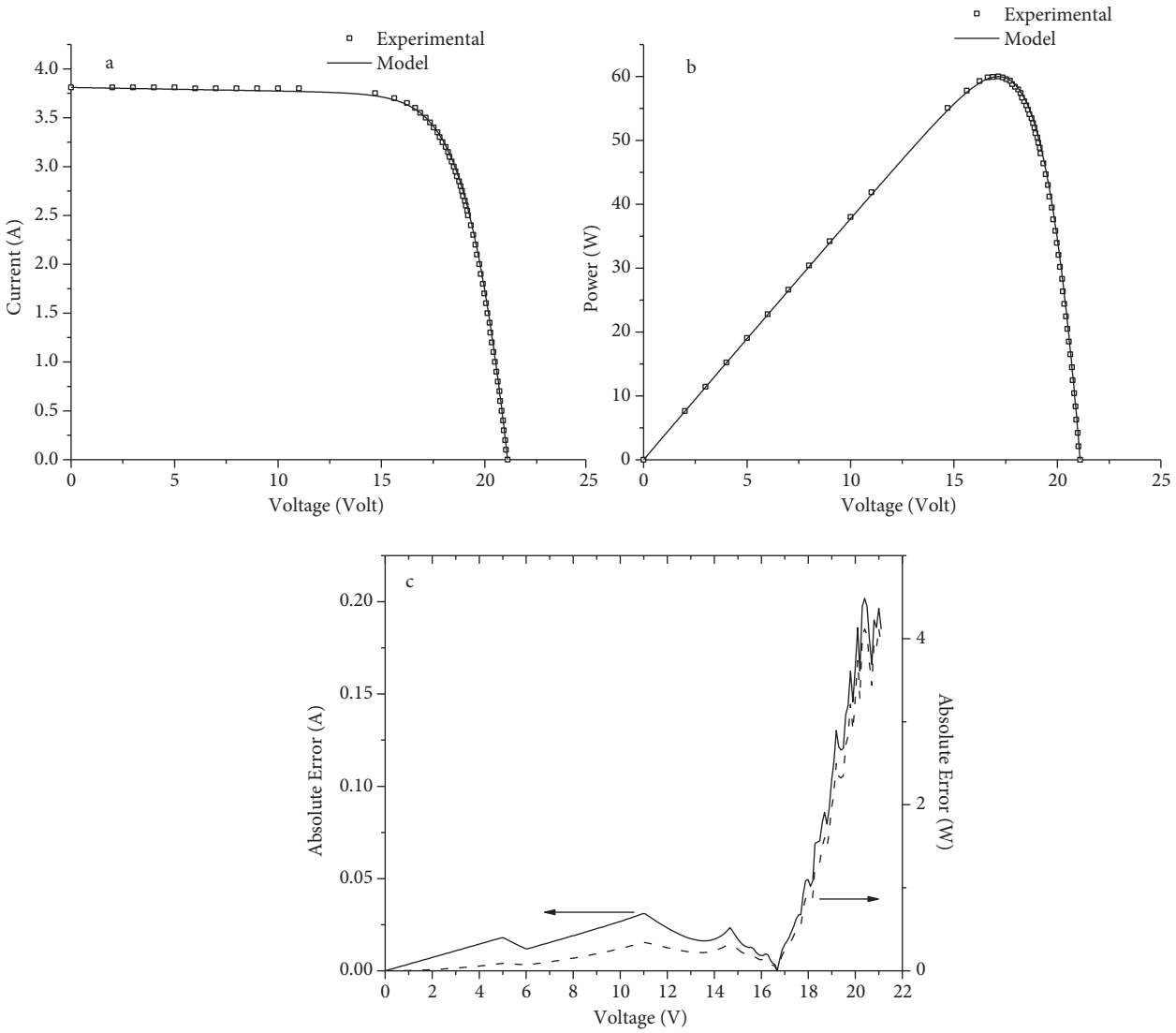

Figure 7. MSX60 solar module at 25 °C, 1000 W/m^2. (a) Current versus voltage characteristics. (b) Power versus voltage characteristics. (c) The variations of absolute errors of current and power with respect to voltage. In (a) and (b) points are experimental data, line is calculated data.

3.2.3. KC200GT solar module

The next selected module is the KC200GT high efficiency multicrystal photovoltaic module by the Kyocera Corporation with 54 cells connected in series [33,34]. The electrical characteristics I_{sc}, V_{oc}, I_{mp}, and V_{mp} shown in Table 1 are provided by the manufacturer's specification sheet. These characteristics are applied to the proposed method and the extracted parameters are listed in Table 2. The mathematical curves for current–voltage and power–voltage fit the experimental data perfectly as illustrated in Figures 8a and 8b. Figure 8c shows the absolute errors of current and power with respect to voltage.

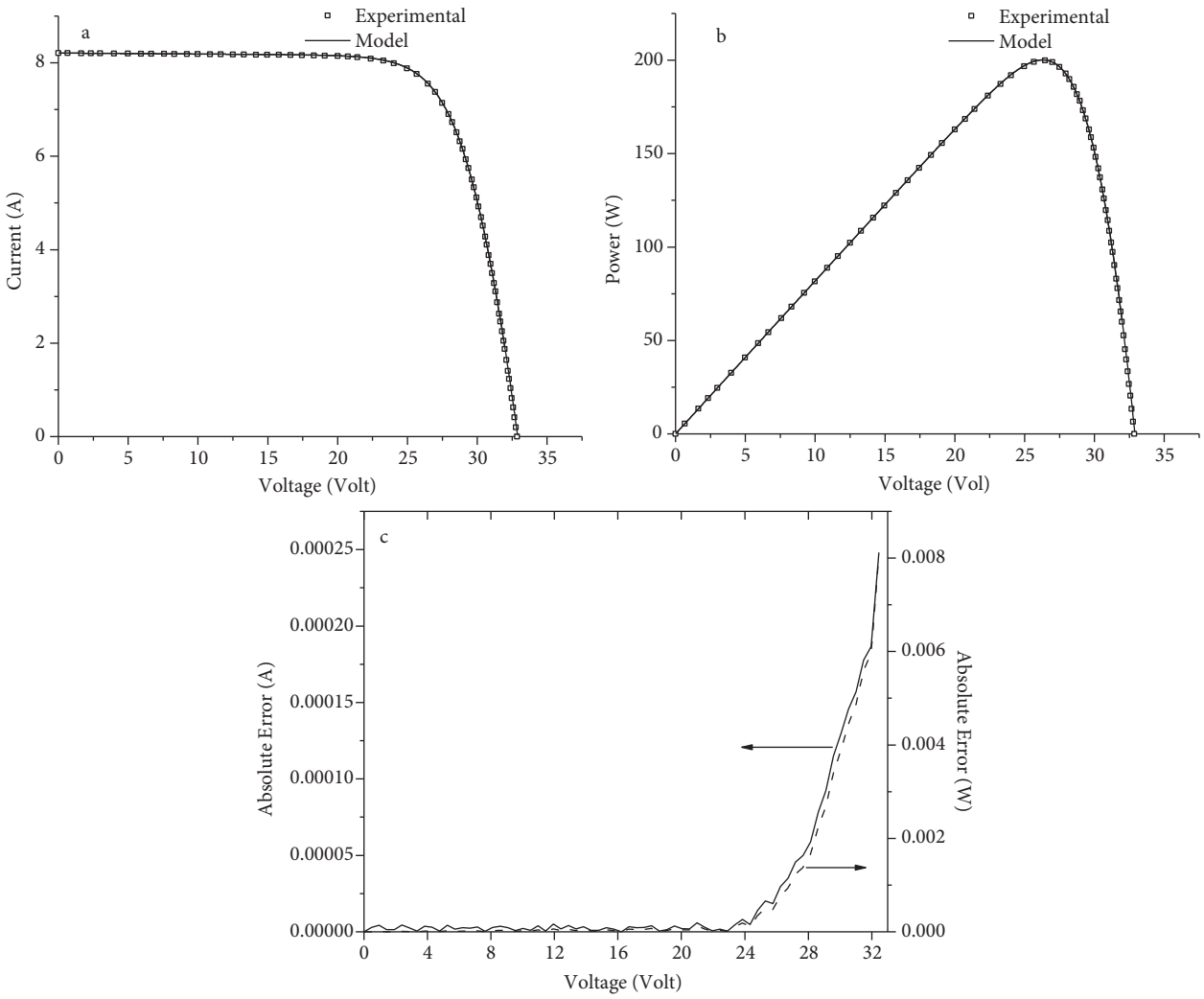

Figure 8. KC200GT solar array at 25 °C, 1000 W/m^2. (a) Current–voltage characteristics. (b) Power–voltage characteristics. (c) Absolute errors of current and power variations with respect to voltage. In (a) and (b) points are experimental data, line is calculated data.

3.3. Application to an organic solar cell

Organic solar cells are generally characterized by 2–4 orders of magnitude larger series resistance values and by smaller shunt resistance values than classical silicon solar cells [24,29]. The photocurrent in organic solar cells is generally about 1000 times smaller than for classical silicon cells [24]. However, the current approach is adapted well to analysis of an organic solar cell. An example of an organic solar cell is presented in Figure 9a. It is clear that the theoretical $I-V$ curve obtained by using the calculated parameters (see Table 2) is in good agreement with the experimental curve obtained from the literature [15]. Figure 9b shows that the calculated $P-V$ characteristics are also in good agreement with the experimental $P-V$ characteristics. The agreement between the calculation results and the experimental data indicates that the proposed method is suitable not only for a silicon solar cell but also for organic solar cells. Figure 9c illustrates the absolute errors of current and power with respect to voltage.

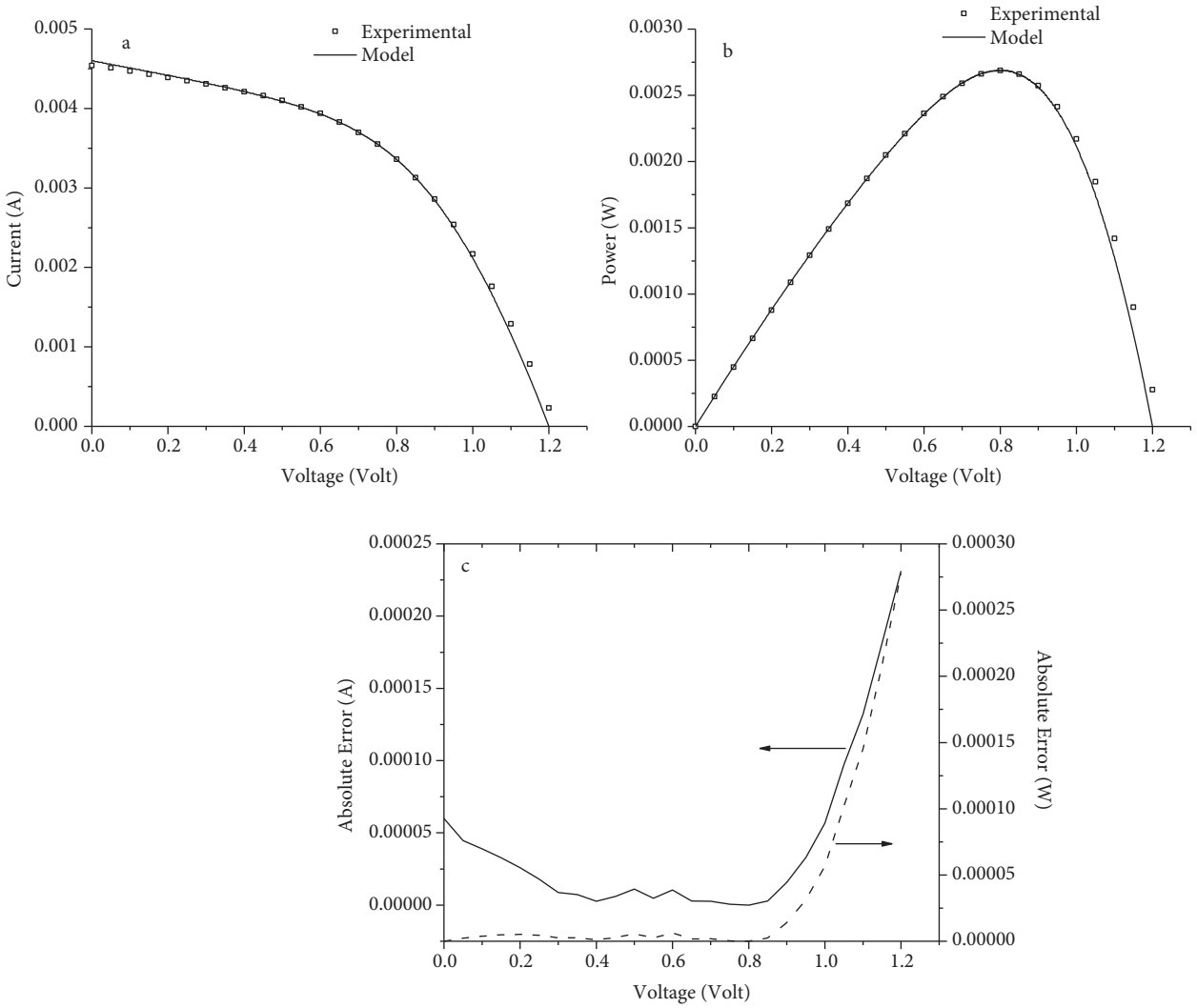

Figure 9. An organic solar cell at 20 °C, 1000 W/m^2. (a) $I-V$ characteristics. (b) $P-V$ characteristics. (c) The variations of absolute errors of current and power with respect to voltage. In (a) and (b) points are experimental data, line is calculated data.

3.4. Application to a DSSC solar cell

Finally, the proposed method is applied to a dye sensitized solar cell (DSSC). The experimental data of a DSSC are obtained from a previous work [19]. In that work, the method requires that the parameter a is fixed to some constant value and then the other parameters are extracted. However, any method that requires fixing an unknown parameter can never yield accurate values of the other parameters. Another study [15] can extract all the parameters, but it requires that the experimental $I-V$ data must be smooth enough, and thus these data have to be approximated by a ninth-degree polynomial expression [15]. Compared to these previous investigations, the current method can be used directly to extract the parameters from raw data. Figure 10a shows that the $I-V$ experimental and the mathematical curves are matched well. Furthermore, Figure 10b shows that the experimental and the calculated $P-V$ curves are in agreement. Figure 10c shows the variations of absolute errors of current and power with respect to voltage.

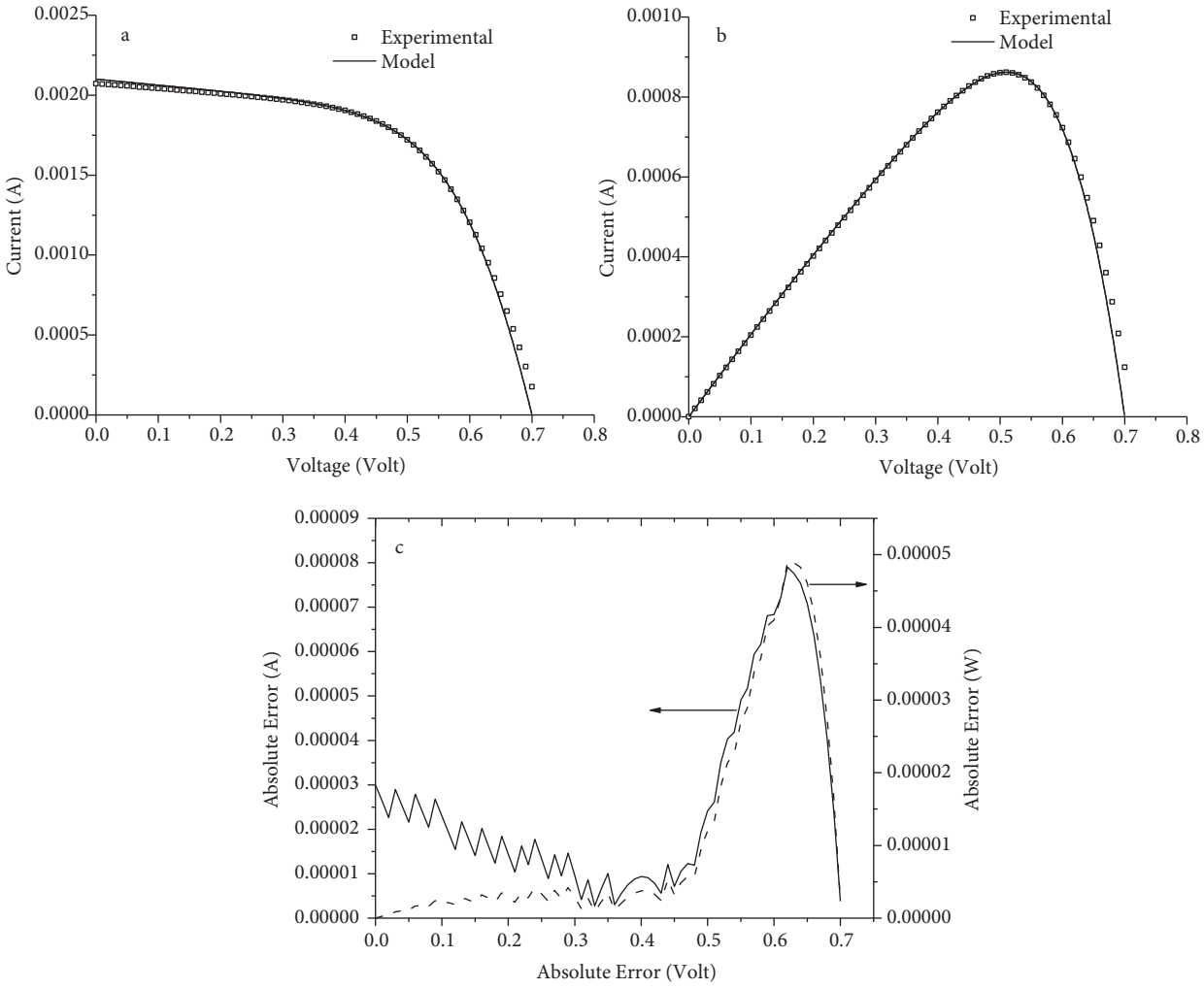

Figure 10. A DSSC solar cell at 20 °C, 1000 W/m^2. (a) $I-V$ curves. (b) $P-V$ curves. (c) The variations of absolute errors of current and power with respect to voltage. In (a) and (b) points are experimental data, line is calculated data.

4. Conclusions

In this article a method based on the Lambert W function approach is applied to analysis of various types of solar cells and modules at a given insolation level and temperature. The experimental data of the PV devices were obtained from the literature. Some of these devices are silicon solar cells and modules in addition to organic and DSSC solar cells. The calculated parameters I_{ph}, I_o, a, R_s, and R_{sh} are in good agreement with those obtained in the literature. The model's $I-V$ characteristics and $P-V$ characteristics are found to be in good agreement with the experimental data.

References

[1] Lopes, L. A. C.; Lienhardt, A. M. In *Power Electronics Specialist, 2003. PESC'03. IEEE 34th Annual Conf. 4*, 2003, p. 1729.

[2] Bouzidi, K.; Chegaar, M.; Nehaoua, N. In *4th International Conf. on Computer Integrated Manufacturing CIP'* 2007, Setif, Algeria, 2007, p. 1.

[3] Araujo, G. L.; Sanchez, E.; Marti, M. *Sol. Cells* **1982**, *5*, 199–204.

[4] Mazhari, B. *Sol. Energy Mater. Sol. Cells* **2006**, *90*, 1021–1033.

[5] Nishioka, K.; Sakitani, N.; Uraoka, Y.; Fuyuki, T. *Sol. Energy Mater. Sol. Cells* **2007**, *91*, 1222–1227.

[6] Pysch, D; Mette, A; Glunz, S. W. *Sol. Energy Mater. Sol. Cells* **2007**, *91*, 1698–1706.

[7] Wolf, M; Rauschenbach, H. *Adv. Energy Convers.* **1963**, *3*, 455–479.

[8] Handy, R. J. *Solid-State Electron.* **1967**, *10*, 765–775.

[9] Servaites, J. D.; Yeganeh, S.; Marks, T. J.; Ratner, M. A. *Adv. Funct. Mater.* **2010**, *20*, 97–104.

[10] Rajkanan, K.; Shewchun J. *Solid-State Electron.* **1979**, *22*, 193–197.

[11] Radziemska, E. *Energy Convers. Manage.* **2005**, *46*, 1485–1494.

[12] Hussein, R.; Borchert, D.; Grabosch, G.; Fahrner, W. R. *Sol. Energy Mater. Sol. Cells* **2001**, *69*, 123–129.

[13] Mialhe, P.; Khoury, A.; Charles, J. P. *Phys. Status Solidi A* **1984**, *83*, 403–409.

[14] Schilinsky, P.; Waldauf, C.; Hauch, J.; Brabec, C. J. *J. Appl. Phys.* **2004**, *95*, 2816–2819.

[15] Ishibashi, K.; Kimura, Y.; Niwano, M. *J. Appl. Phys.* **2008**, *103*, 094507-094507-6.

[16] Easwarakhanthan, T.; Bottin, J.; Bouhouch, I.; Boutrit, C. *Int. J. Sol. Energy* **1986**, *4*, 1–12.

[17] Chegaar, M.; Ouennoughi, Z.; Hoffmann, A. *Solid-State Electron.* **2001**, *45*, 293–296.

[18] Kaminski, A.; Marchand, J. J.; Laugier, A. *Solid-State Electron.* **1999**, *43*, 741–745.

[19] Murayama, M.; Mori, T. *Jpn. J. Appl. Phys.* **2006**, Part 1 *45*, 542–545.

[20] Jain, A.; Kapoor, A. *Sol. Energy Mater. Sol. Cells* **2005**, *86*, 197–205.

[21] Ortiz-Conde, A.; Garcia Sanchez, F. J. *Solid-State Electron.* **2005**, *49*, 465–472.

[22] Ding, J.; Radhakrishnan, R. *Sol. Energy Mater. Sol. Cells* **2008**, *92*, 1566–1569.

[23] Ortiz-Conde, A.; Garcia Sanchez, F. J.; Muci, J. *Sol. Energy Mater. Sol. Cells.* **2006**, *90*, 352–361.

[24] Zhang, C.; Zhang, J.; Hao, Y.; Lin, Z.; Zhu, C. *J. Appl. Phys.* **2011**, *110*, 064504–064511.

[25] Aazou, S.; Assaid, E.M, *Global Journal of Physical Chemistry* **2011**, *2*, 61–67.

[26] http://www.maplesoft.com/applications/view.aspx?SID=33045.

[27] Ghani, F.; Duke, M. *Solar Energy* **2011**, *85*, 2386–2394.

[28] Ghani, F.; Duke, M.; Carson, J. *Solar Energy* **2013**, *91*, 422–431.

[29] Chegaar, M; Azzoouzi, G.; Mialhe, P. *Solid-State Electron* **2006**, *50*, 1234–1237.

[30] Kennerud, K. *IEEE Trans. Aerospace and Electronic Systems.* AES-5 **1969**, *6*, 912–917.

[31] El Tayyan, A. A. *Journal of Electron Devices* **2011**, *9*, 335–341.

[32] Solar Electric Supply. "MSX-60 60 Watt & MSX-64 64 Watt." Internet: http://www.solarelectricsupply.com, [August 20, 2011].

[33] Villalva, M. G.; Gazoli, J. R.; Filho, E. R. *Brazilian Journal of Power Electronics* **2009**, *14*, 35–45.

[34] Kyocera Corporation. "Model KC200GT." Internet: http://www.txspc.com, [August 21, 2011].